European Journal of Orthodontics 31 (2009) 613–619
doi:10.1093/ejo/cjp043
Advance Access Publication 21 July 2009

A cross-sectional study on the relationship between craniofacial morphology and the coronoid process

Takahiro Torisu*, Kazuhiro Yamada**, Tadao Fukui*, Masaki Yamaki*, Junichi Nakamura* and Isao Saito*
*Division of Orthodontics, Niigata University Graduate School of Medical and Dental Sciences, Chuo-ku, Niigata and **Department of Orthodontics, School of Dentistry, Matsumoto Dental University, Shiojiri, Nagano, Japan

SUMMARY Although there have been some reports on the relationship between craniofacial morphology and the activity of the temporal muscle attached to the coronoid process, such relationship is still unclear. The aim of the present study was therefore to investigate the relationship between the coronoid process and overall craniofacial morphology using lateral cephalograms of 60 female subjects (mean age 9.6 years) without mandibular deviation. Statistical testing was undertaken using stepwise regression analysis.

Anterior coronoid marginal depth correlated negatively ($r = 0.71$) with gonial angle, SNA, and overjet. The coronoid angle also correlated negatively ($r = 0.86$) with both the vertical and horizontal lengths from sella to the coronoid tip as well as with the horizontal length from sella to the posterior ramus margin. Furthermore, the coronoid length correlated positively ($r = 0.61$) with the coronoid angle and the anterior coronoid marginal depth. The coronoid width was also positively ($r = 0.69$) correlated with overbite.

Coronoid process morphology is related not only to mandibular morphology and position but also to maxillary position and the dental relationship in the anterior region. It therefore seems clear that coronoid process morphology might be related to temporal muscle functioning and its associated craniofacial morphological measurements.

Introduction

Since it is essential to predict craniofacial growth, especially mandibular growth, in subjects undergoing orthodontic treatment, many studies have reported on the relationship between mandibular morphology and craniofacial growth (Enlow and Harris, 1964; Moss, 1968). The mandible consists of membranous bone and its growth is influenced by functioning of the attached muscles (Enlow and Harris, 1964; Pirttiniemi, 1998). Conversely electromyographic (EMG) studies of the temporal muscle attached to the coronoid process have revealed that temporal muscle activity during clenching correlates negatively with the mandibular plane, gonial angles, and overjet and positively with overbite (Lowe, 1980; Petrofsky and Lind, 1980; Niide *et al.*, 1986; Kouno and Sato, 1995; Blanksma *et al.*, 1997). It has also been reported that the anterior portion of the temporalis is especially active during biting and that the posterior portion of the temporalis is involved in maintaining mandibular position (Lowe, 1980; Kouno and Sato, 1995; Pirttiniemi, 1998). Although functioning of the temporal muscle attached to the coronoid process influences craniofacial morphology, the relationship between overall craniofacial morphology and the coronoid process has not yet been clearly elucidated. The aim of the present study was therefore to investigate the relationship between the coronoid process and general craniofacial morphology using lateral cephalograms.

Materials and methods

Of 368 orthodontic patients who sought orthodontic treatment at Niigata University Dental Hospital from 1992 to 2002, 60 subjects satisfied the inclusion criteria of having no deformities or clinically defined mandibular deviations [deviations of 3 mm or more on the postero-anterior (PA) cephalograms]. The lateral and PA cephalograms (magnification 1:1.1) were obtained with vertically adjustable head holders in the intercuspal position and traced by the same author (TT). All procedures were approved by the Niigata University Institutional Review Board.

Thirteen skeletal landmarks were identified on the lateral cephalograms (Figure 1) and measurements of the eight angular and 10 linear were carried out (Table 1). In particular, the coronoid process measurements (Figure 2) were defined as follows:

First, a vertical line perpendicular to the Frankfort horizontal plane was drawn through point P (the most anterior point on the anterior surface of the mandibular ramus).

Line CD, from the deepest point of the mandibular notch (C) to the most posterior point on the mandibular ramus (D), was defined as the coronoid base. The furthest point on the coronoid process from this coronoid base was defined as Cor.

Line A: a line perpendicular to the Frankfort horizontal plane through point D.

Line B: a line perpendicular to the Frankfort horizontal plane through point P.

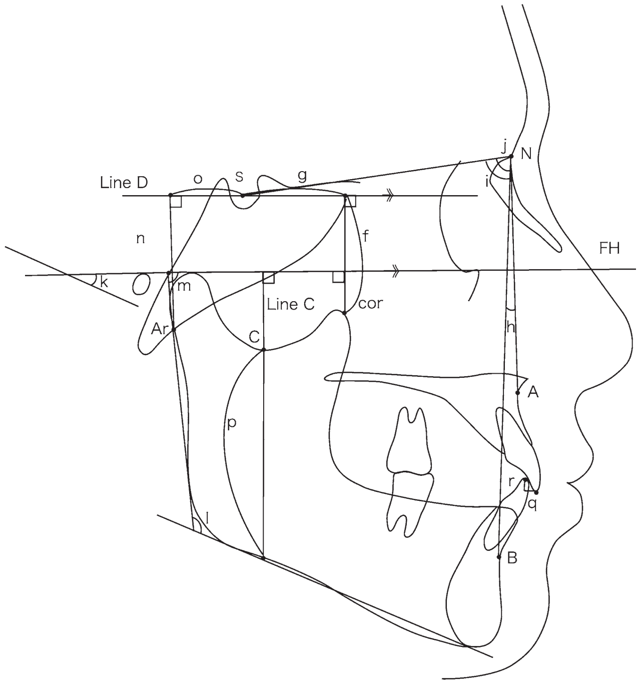

Figure 1 Cephalometric measurements. f: coronoid (cor)-vertical length, g: cor-antero-posterior length; h: ANB i: SNA j: SNB; k: mandibular plane angle, l: gonial angle, m: ramus inclination angle; n: Ar-vertical length, o: Ar-anterior posterior length, p: m-vertical length; q: overjet, r: overbite; Line C: a line perpendicular to the Frankfort horizontal plane through point C; Line D: a line parallel to the Frankfort horizontal plane through sella; Vertical Cor distance (f): the perpendicular distance from line D to Cor; Antero-posterior Cor position (G): the length from sella, along line LC parallel to the Frankfort horizontal plane through sella to its intersection with the perpendicular line through the Cor; Vertical Ar length (n): the distance perpendicular line D to point Ar (the intersection point of the ramus and the cranial base); Antero-posterior Ar length (o): the antero-posterior distance from sella along line D to its intersection with the perpendicular line through Ar.

Table 1 Values for lateral cephalometric measurements of 60 subjects.

	Mean	Standard deviation	Maximum	Minimum
a: cor-notch (mm)	4.1	1.3	6.5	1.0
b: cor-angle (°)	60.9	7.9	80.0	43.0
c: cor-length (mm)	18.8	2.3	23.0	14.0
d: h-widge (mm)	10.4	1.4	13.0	8.0
e: s-angle (°)	158.2	9.1	180.0	138.0
f: cor-vertical (mm)	24.0	3.8	34.0	17.0
g: cor-antero-posterior (mm)	22.9	3.7	30.0	11.0
h: ANB (°)	3.5	2.5	8.0	−2.0
i: SNA (°)	80.2	3.1	91.0	73.0
j: SNB (°)	76.7	3.5	85.0	70.0
k: Mp (°)	28.4	4.8	42.0	19.0
l: Go (°)	126.3	5.8	136.0	113.0
m: Ri (°)	81.9	4.0	92.0	70.0
n: R-vertical (mm)	29.5	2.3	35.0	24.0
o: R-antero-posterior (mm)	16.7	3.5	24.0	8.0
p: m-vertical (mm)	42.0	2.9	49.0	35.0
q: overjet (mm)	2.9	3.0	9.5	−6.0
r: overbite (mm)	3.1	2.4	14.0	0.0

The coronoid notch depth was defined as the perpendicular distance between lines A and B.

The coronoid length was defined as the distance from point Cor to the midpoint (point E) between C and D on line CD (Ricketts *et al.*, 1972).

The coronoid width was defined as the length of the line C′D’ parallel to CD through H (the midpoint of the coronoid length above).

Coronoid angle: the angle formed by the intersection of the Frankfort horizontal plane and the Cor–E line.

Coronoid curvature: the angle formed at point G (the midpoint of the coronoid width) between the lines drawn from G to Cor and E.

In order to obtain the regression equation for the position, angle, and length of the coronoid process, a stepwise regression analysis incremental method (Tamari *et al.*, 2003) was performed on the following five measurements:

1. Coronoid notch depth
2. Coronoid angle

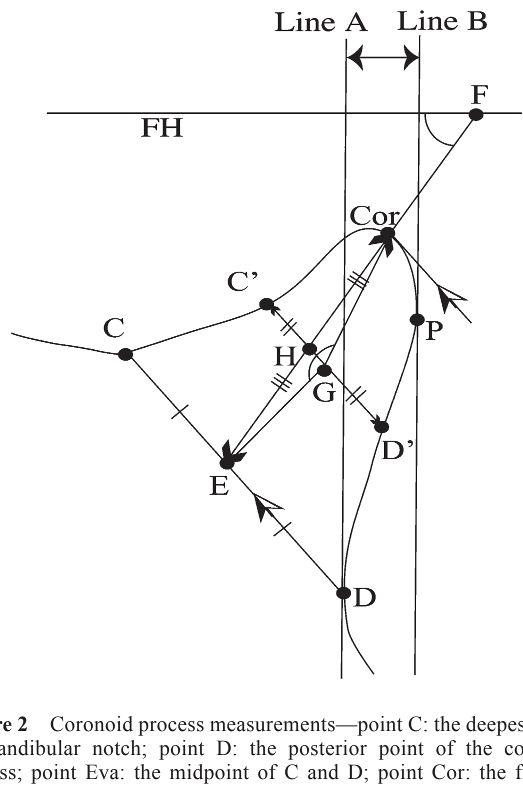

Figure 2 Coronoid process measurements—point C: the deepest point of mandibular notch; point D: the posterior point of the coronoid process; point Eva: the midpoint of C and D; point Cor: the furthest point on the coronoid process from the coronoid base; line C′D′: the length of the line parallel to CD through the midpoint of the coronoid length (point H); point F: the intersection of the Frankfort plane and Cor–Eva line; point G: the midpoint of C′ and D′; coronoid curvature (E–G–Cor angle) coronoid notch depth (H1–H2 length); coronoid angle (FH–F–E angle); coronoid length (E–Cor length); and coronoid width (C′D′ length).

3. Coronoid length
4. Coronoid width
5. Coronoid curvature

(adoption F value = 4, exclusion F value = 3.996) using the StatView program (SAS Institute Inc., Cary, North Carolina, USA).

Moreover, the significance of the multiple correlation coefficient, r, was assessed by the F distribution.

Method error

Errors in landmark localization during tracing were evaluated by having the same researcher retrace each of the lateral cephalograms three times, with an interval of 1 week between tracing. The method error was assessed using the formula of Dahlberg (Houston, 1983) on 15 pairs of measurements randomly selected from the data. For angular cephalometric error measurements ranged from 0.43 to 0.88 degrees and linear measurement error from 0.77 to 0.88 mm. Six cephalograms with unclear coronoid process images were excluded.

Results

Measurement value correlations

The correlations between the various measurements were calculated (Table 2). Significant correlations were found for coronoid process morphology with craniofacial morphology; coronoid notch depth with both ANB and antero-posterior Ar length; coronoid angle correlated with ANB and vertical Ar length; antero-posterior Ar length with overjet; coronoid length with ANB also significantly correlated; coronoid angle with coronoid length, width, curvature, height (vertical length), and antero-posterior length; coronoid curvature with vertical coronoid length; ANB angle with Ar height (vertical Ar length), antero-posterior Ar length, overjet, and overbite; gonial angle with mandibular plane angle and ramus inclination; ramus inclination itself with ramus height; and antero-posterior Ar length with both overjet and overbite.

Regression equation

Stepwise regression analysis showed the following multiple regression equations and multiple correlation coefficients for the five coronoid measurements (Tables 3 and 4).

Coronoid notch depth

$$y = -0.101\mathrm{Xt} + 0.25\mathrm{Xu} - 0.058\mathrm{Xq} - 0.124\mathrm{Xm} - 0.152\mathrm{Xg} - 0.055\mathrm{Xw} + 31.949,$$

where Xt = coronoid angle, Xu = coronoid length, Xq = gonial angle, Xm = SNA, Xg = overjet, Xw = coronoid curvature, $r = 0.71$.

Coronoid angle

$$y = -1.514\mathrm{Xs} + 1.03\mathrm{Xu} - 0.432\mathrm{Xa} - 0.678\mathrm{Xd} - 0.705\mathrm{Xb} - 0.247\mathrm{Xw} + 124.492,$$

where Xs = coronoid notch depth, Xu = coronoid length, Xa = vertical Cor length, Xd = antero-posterior Ar length, Xb = antero-posterior Cor length, Xw = coronoid curvature, $r = 0.84$.

Coronoid length (u)

$$y = 0.658\mathrm{Xs} + 0.156\mathrm{Xt} + 6.669,$$

where Xs = coronoid notch depth, Xt = coronoid angle, $r = 0.59$.

Coronoid width (v)

$$y = 0.099\mathrm{Xt} + 0.174\mathrm{Xh} + 4.033,$$

where Xt = coronoid angle, Xh = overbite, $r = 0.47$.

Coronoid curvature (w)

$$y = -1.659\mathrm{Xs} - 0.61\mathrm{Xt} + 0.48\mathrm{Xp} + 215.992,$$

where Xs = coronoid notch depth, Xt = coronoid angle, Xp = mandibular plane angle, $r = 0.64$.

The results of a stepwise regression analysis for each of the above measurements are shown in Table 4. Both the multiple correlation coefficients (Table 3) and standard regression coefficients (Table 4) for each of these measurements were significant.

Discussion

Previous studies have shown that activity in the temporal muscle attached to the coronoid process is related to craniofacial morphology (Lowe 1980; Kouno and Sato, 1995; Pirttiniemi, 1998), which suggests that high temporal muscle activity is associated with a low mandibular plane angle, a large overbite, and a small overjet. However, there have been no reports concerning the relationship between the coronoid process and craniofacial morphology. In the present study, their correlation was investigated using stepwise analysis (dependent variables: the length, direction, width, curvature, and anterior marginal depth of the coronoid process; independent variables: craniofacial and other coronoid process measurements).

Coronoid notch depth

Stepwise analysis showed that coronoid notch depth became deeper with an increase in gonial angle, SNA, and overjet: typical morphological characteristics of Class II subjects with a high angle and low masticatory activity (Isberg, 1990). EMG studies have demonstrated that both overjet

Table 2 Correlation matrix between each measurement.

	cor-notch	cor-angle	cor-length	h-width	s-angle	cor-vertical	Antero-posterior-cor	ANB	SNA	SNB	Mp	Go	Ri	R-vertical	Antero-posterior-R	Vertical-m	Overjet	Overbite
a: cor-notch	1																	
b: cor-angle	−0.079	1																
c: cor-length	0.309*	0.409**	1															
d: h-width	−0.239	0.381**	0.15	1														
e: s-angle	−0.189	−0.598**	−0.094	−0.175	1													
f: cor-vertical	0.012	−0.565**	−0.271*	−0.361*	0.38**	1												
g: antero-posterior-cor	−0.261	−0.44**	−0.038	−0.166	0.332*	0.116	1											
h: ANB	−0.289**	−0.507**	−0.405**	−0.103	0.318*	0.357**	−0.505	1										
I: SNA	−0.264	−0.013	0.039	0.178	0.093	0.325	-1.56×10^{-1}	0.22	1									
j: SNB	−0.028	0.347**	0.321*	0.229	−0.143	0.033	0.22	−0.514**	0.723**	1								
k: Mp	0.011	0.024	−0.128	−0.222	0.268*	−0.138	−0.178	0.143	−0.275*	−0.343*	1							
l: Go	−0.18	0.227	−0.045	−0.044	−0.29*	−0.44**	−0.204	−0.099	−0.231	−0.133	0.707**	1						
m: Ri	0.256	−0.337*	−0.094	−0.145	0.134	0.491**	−0.185	0.306*	0.021	−0.198	0.077	−0.615**	1					
n: R-vertical	−0.208	−0.36**	−0.229*	0.104	0.209	0.491**	−0.369	0.527**	0.307	−0.103	0.088	−0.114	0.287*	1				
o: antero-posterior-R	−0.315**	−0.432**	−0.334	−0.084*	0.274*	0.361	−0.728	0.521**	0.04	−0.333*	0.127	0.004	0.137	0.244	1			
p: vertical-m	0.058	−0.333*	−0.101	0.146	0.163	0.153	−0.061	0.301*	0.012	−0.203	0.013	−0.278*	0.42**	0.169	0.213	1		
q: overjet	−0.305*	−0.406**	−0.215	−0.122	0.328*	0.282	−0.322	0.434**	0.01	−0.298*	−0.068	−0.136	0.129	0.207	0.398**	0.142	1	
r: overbite	−0.131	−0.326*	−0.3*	0.126*	0.152	0.282	−0.235	0.397**	−0.026	−0.304*	−0.182	−0.251	0.199	0.234	0.357**	0.224	0.263	1

*$P < 0.05$; **$P < 0.001$.

Table 3 Stepwise regression analysis.

Dependent variable	Explanatory variable	R	R^2	Standard error for dependent variables	Multiple regression equation	F value
a	b c l I q e	0.71	0.5	6.485	$y = -0.1Xb + 0.246Xc - 0.059Xl - 0.126Xi - 0.147Xq - 0.064Xe + 33.737$	7.947**
b	a c f o g e	0.86	0.74	12.173	$y = -1.554Xa + 1.054Xc - 0.409Xf - 0.688Xo - 0.661Xg - 0.307Xe + 132.593$	22.242**
c	a b e	0.613	0.375	8.078	$y = 0.783Xa + 0.2Xb - 0.1Xe - 12.565$	10.02**
d	b k n f p	0.686	0.47	3.899	$y = 0.067Xb - 0.096Xk + 0.261Xn - 0.164Xf + 0.127Xp - 0.073$	8.516**
e	a b c k	0.729	0.532	10.384	$y = -2.33Xa - 0.849Xb - 1.1Xc + 0.402Xk + 210.277$	13.906**

**$P < 0.001$.

Table 4 Results of stepwise regression analysis.

	Regression coefficient	Standard error	Standard regression coefficient	F-to-remove
Independent variables for coronoid notch				
Intercept	31.949	6.492	31.949	24.221
b: cor-angle	−0.101	0.024	−0.581	17.514
c: cor-length	0.25	0.065	0.449	14.71
l: Go	−0.058	0.025	−0.264	5.655
i: SNA	−0.124	0.043	−0.302	8.201
q: overjet	−0.152	0.049	−0.358	9.786
e: cor-curvature	−0.055	0.019	−0.354	8.08
Independent variables for coronoid angle				
Intercept	124.492	13.472	122.492	85.393
a: cor-notch	−1.514	0.525	−0.264	8.332
c: cor-length	1.03	0.288	0.322	12.743
f: cor-vertical	−0.432	0.185	−0.215	5.483
o: Ar-antero-posterior	−0.678	0.202	−0.321	11.262
g: cor-antero-posterior	−0.705	0.182	−0.345	14.943
e: cor-curvature	−0.247	0.081	−0.279	9.357
Independent variables for coronoid length				
Intercept	6.669	2.397	6.669	7.743
a: cor-notch	0.658	0.204	0.367	10.41
b: cor-angle	0.156	0.036	0.5	19.351
Independent variables for coronoid width				
Intercept	4.033	1.709	4.033	5.5690
b: cor-angle	0.099	0.026	0.491	13.955
r: overbite	0.174	0.083	0.277	4.445
Independent variables for coronoid curvature				
Intercept	215.992	9.895	215.992	476.497
a: cor-notch	−1.659	0.709	−0.256	5.47
b: cor-angle	−0.61	0.124	−0.54	24.4
k: Mp	0.402	0.191	0.211	6.352

and gonial angle are negatively correlated with activity in the anterior part of the temporal muscle during maximum clenching (Lowe 1980; Kouno and Sato, 1995; Pirttiniemi, 1998). In subjects with a retruded maxilla, the mandible might adapt to this posterior maxillary position by morphological changes including a deeper coronoid notch depth as a result of greater temporal muscle activity. Due to the different maxillomandibular relationships in subject with a large overjet/protruded maxilla versus those with a small overjet/protruded maxilla, it seems reasonable to suppose that they might also display differing mandibular movement patterns during mastication. Because the temporal muscle attached to the coronoid process has the function of adjusting the mandibular position during mastication, the coronoid notch depth might change to adapt to different mandibular movement patterns. However, details on mandibular movement patterns due to such differences of maxillomandibular position still remain unclear. Further studies investigating the relationships between coronoid process morphology, maxillary position, and masticatory patterns are required.

The anterior part of the temporal muscle is attached to the anterior part of the coronoid process and is also active during maximum clenching (Lowe, 1980; Petrofsky and Lind, 1980; Terada and Sato, 1982; Kouno and Sato, 1995). Therefore, it might be hypothesized that in subjects with increased muscular

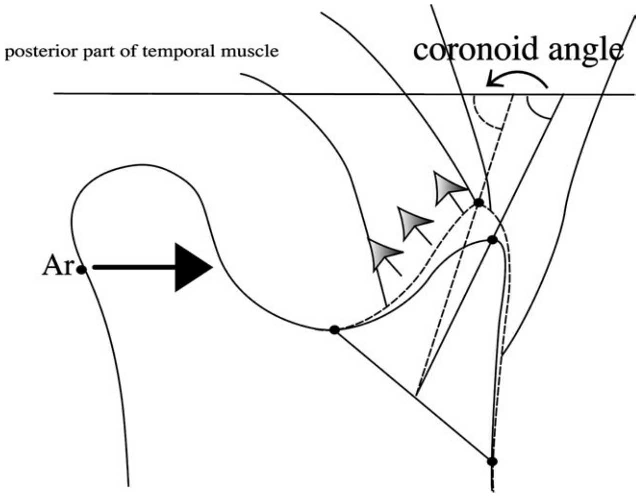

Figure 3 The relationship between coronoid process morphology and the posterior part of temporal muscle. When the mandible is positioned anteriorly (black arrow), the posterior part of the temporal muscle pulls the mandible posteriorly (grey arrows), providing mandibular stability. This muscle tension results in the coronoid process becoming more vertical with an increase in the coronoid process curvature.

activity during maximum clenching, bone formation on the anterior marginal surface of the coronoid process increases, resulting in an increase in anterior coronoid notch depth.

Coronoid angle

The coronoid process became more vertical as the posterior edge of the ramus (Ar) moved anteriorly and was accompanied by an increase in coronoid process curvature.

When the mandible was positioned anteriorly, the posterior part of the temporal muscle pulled the mandible posteriorly, providing mandibular stability (Figure 3; Lowe, 1980; Petrofsky and Lind, 1980; Terada and Sato, 1982; Kouno and Sato, 1995). This muscle tension resulted in the coronoid process becoming more vertical, with an increase in coronoid process curvature.

Coronoid length

Coronoid length significantly increased with an increase in coronoid anterior notch depths as well as increasing coronoid process angles. As mentioned, an increase in bone formation at the anterior, superior, and posterior parts of the coronoid process might occur due to the activity of the anterior and posterior parts of the temporal muscle (Figures 3 and 4). Therefore, an increase in coronoid process length probably occurs due to the functioning of these anterior and posterior parts of the temporal muscle.

Coronoid width

Stepwise analysis showed that the coronoid width increased in proportion to the increase in overbite. EMG studies have

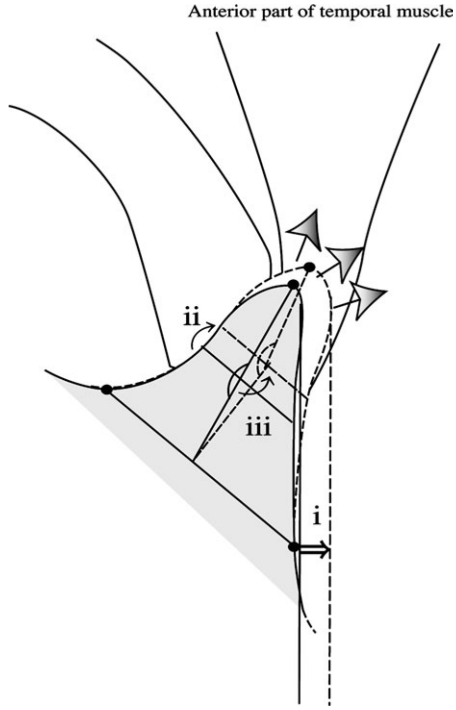

Figure 4 The relationship between coronoid process morphology and the anterior part of the temporal muscle. i: coronoid notch depth; ii: coronoid width; and iii: coronoid curvature. Stepwise analysis showed that coronoid length increases with an increase in the coronoid anterior notch depth and the coronoid process angle. An increase in bone formation on the anterior, superior, and posterior parts of the coronoid process might occur due to the activity of the anterior and posterior parts of the temporal muscle (grey arrows).

demonstrated a relationship between overbite and activity in the anterior part of the temporal muscle and the masseter during maximum clenching (Enlow and Harris 1964; Lowe, 1980; Petrofsky and Lind, 1980). It therefore seems that both overbite and coronoid process width increase in relation to the increase in activity of the anterior part of the temporal muscle.

Coronoid curvature

Coronoid curvature decreased in proportion to the decrease in mandibular plane angle. Previous EMG studies have demonstrated negative correlations between temporal and masseter muscle activity and the mandibular plane angle (Lowe, 1980; Petrofsky and Lind, 1980; Niide *et al.*, 1986). The anterior part of the temporal muscle attached to the anterior part of the coronoid process has been found to be active during maximum clenching (Terada and Sato, 1982; Kouno and Sato, 1995). It is therefore possible that in subjects with small mandibular plane angles, bone formation occurs on the anterior part of the coronoid process at the attachment of the temporal muscle. Since the midpoint of the coronoid process width (point G) in the present subjects with small mandibular plane angles was positioned more anteriorly, this may have been responsible for the increase in their coronoid curvature.

Conclusions

The present study showed the following:

1. Anterior coronoid marginal depth correlated negatively with gonial angle, SNA, and overjet.
2. Coronoid angle also correlated negatively with the vertical and horizontal lengths from sella to the coronoid tip as well as the horizontal length from sella to the posterior ramus margin.
3. Coronoid length correlated positively with both the coronoid angle and anterior coronoid marginal depth.
4. Coronoid width was also positively correlated with overbite.

Coronoid process morphology was therefore found to be related not only to mandibular morphology and position but also to the position of the maxilla and the relationship of the dentition.

Address for correspondence

Takahiro Torisu
Division of Orthodontics
Niigata University Graduate School of Medical and Dental Sciences
2-5274 Gakkocho-dori
Chuo-ku
Niigata 951-8514
Japan
E-mail: toritaka@dent.niigata-u.ac.jp

References

Blanksma N G, Van Eijden T M, van Ruijven L J, Weijs W A 1997 Electromyographic heterogeneity in the human temporalis and masseter muscles during dynamic tasks guided by visual feedback. Journal of Dental Research 76: 542–551

Enlow D H, Harris D B 1964 A study of the postnatal growth of the human mandible. American Journal of Orthodontics 50: 25–50

Houston W J B 1983 The analysis of errors in orthodontic measurements. American Journal of Orthodontics 83: 382–390

Isberg A 1990 A cephalometric analysis of patients with coronoid process enlargement and locking. American Journal of Orthodontics and Dentofacial Orthopedics 97: 35–40

Kouno S, Sato H 1995 Two different functions in the masticatory muscle during voluntary clenching performances. Dentistry in Japan 32: 60–63

Lowe A A 1980 Correlations between orofacial muscle activity and craniofacial morphology in a sample of control and anterior open-bite subjects. American Journal of Orthodontics 78: 89–98

Moss M L 1968 Functional cranial analysis of mammalian mandibular ramal morphology. Acta Odontologica Scandinavica 71: 423–447

Niide J, Fushima K, Miyagawa Y, Oda H, Suzuki Y 1986 Relationships between masticatory muscle fatigue and dento-facial morphology. Journal of Japanese Orthodontic Society 45: 401–410

Petrofsky J S, Lind A R 1980 Frequency analysis of the surface electromyogram during sustained isometric contractions. European Journal of Applied Physiology and Occupational Physiology 43: 173–182

Pirttiniemi P 1998 Normal and increased functional asymmetries in the craniofacial area. Acta Odontologica Scandinavica 56: 342–345

Ricketts R M, Bench R W, Hilgers J J, Schuhof R 1972 An overview of computerized cephalometrics. American Journal of Orthodontics 61: 1–28

Tamari K, Okuyama Y, Nakasima A 2003 Clinical determination of incisor position and angulation for treatment goal. Study with the good occlusion subjects. Journal of Japanese Orthodontic Society 62: 123–130

Terada S, Sato T 1982 Nerve supply of the medial and lateral pterygoid muscles and its morphological significance. Okajimas Folia Anatomica Japonica 59: 251–264